On the use of liquid metals as cathode in molten fluorides

M. Gibilaro *, S. Bolmont, L. Massot, L. Latapie, P. Chamelot

Université de Toulouse, UPS, CNRS, Laboratoire de Génie Chimique, 118 Route de Narbonne, F-31062 Toulouse, France

A B S T R A C T

The aim of this article is to investigate the behaviour of liquid metallic electrodes in pyroprocesses. Thus, studies of electrochemical properties of various liquid metallic electrodes (Bi, Sb, Sn, Pb, Ga) were performed in LiF–NaF (750 °C) and LiF–CaF_2 (850 °C). Thanks to linear sweep voltammetry technics, electroactivity domains were determined as well as a reactivity (Sb > Bi > Pb > Sn > Ga > Mo) and a nobility scale (Ga < Sn < Pb < Sb < Bi < Mo), valid in both solvent: from these data, the extraction yield of an element can be evaluated. Then the preparation of alloyed cathodes for reductive extraction process, corresponding to a spontaneous reaction between a reducing agent contained in the liquid metal and the element to be removed from the molten salt, was examined. The in situ generation of liquid Bi–Li, Na or Ca (reducing agents) reactive electrodes was performed in LiF–NaF and LiF–CaF_2 solvent by galvanostatic electrolyses. Elementary analyses showed that Li^+ and Ca^{2+} were reduced on Bi at the same reaction rate in LiF–CaF_2, whereas Na was preferentially inserted into Bi, compared to Li, in LiF–NaF. Linear relationships between the electrolysis potential and the logarithm of the global mole fraction of reducing agent were found. As a consequence, by fixing the potential at the end of the electrolysis, Bi reactive cathodes with a controlled quantity of reducing agent can be produced in galvanostatic conditions.

1. Introduction

Pyro-electrometallurgy is commercially used to recover or refine metals, including large scale fabrication for metals, such as liquid aluminium production. The value of using liquid cathode is evidenced by many advantages: a complete physical separation between the electrolyte and the produced metal, a constant surface area of the electrode, and an easier coalescence of microdrops and metallic fog.

Therefore, liquid metals research has being transferred to nuclear applications for pyrochemical reprocessing of irradiated nuclear fuels. In the frame of Partitioning and Transmutation concept (P&T) [1], goals are to reduce the radiotoxicity and the volume of nuclear wastes in the back-end of fuel cycle. Several processes have thus been developed to selectively recover minor actinides from nuclear fuel on a liquid metal cathode. In pyrochemical treatment, the main steps are either the electrorefining or the reductive extraction, based both on a contact between a molten salt and a liquid metallic system. The use of liquid metal electrodes allows a group recovery of metals, captured as an alloyed compound: a safe recovery is then ensured (proliferation resistant) and metals are thermodynamically stabilised. Moreover, diffusion coefficients in the salt and into the liquid metal have the same order of magnitude, e.g. for uranium [2,3] in LiCl–KCl and in Cd at 450 °C: compared to intermetallic diffusion in a solid electrode, diffusion in the liquid is faster.

In the electrorefining process, the metallic fuel is anodically dissolved into a molten salt and most of uranium is selectively recovered on a solid cathode whereas the transuranic elements and uranium are collected on a liquid metallic pool, leaving the fission products in the salt. In Japan, investigations were performed in LiCl–KCl on liquid Cd cathode [4–7] on a wide range of alkaline earths (Sr, Ba...), rare earths (Ce, Nd...) and minor actinides (Np, Am...). Authors determined the activity coefficients, the separation factors, the mass transfer coefficients between the molten salt and the liquid phase. Parallel developments were realised for instance in the US [8–10] and in Korea [11,12] on the same systems.

Concerning the liquid–liquid extraction metallic ions are recovered into a metallic pool directly by electrolysis or using metal reducing agents (RA), as alkaline or alkaline earth elements. In the reductive extraction a spontaneous reaction between RA (oxidation) contained in a liquid metallic pool and the element to be extracted in the salt (reduction) takes place. A transfer of the element is observed from the salt to the liquid electrode in the metallic form. Numerous studies were dedicated to this technique in chloride salts, where Bi [13] and Cd [14] were mainly investigated as metallic pools and compared [15] in LiCl–KCl. Tests on a Zn liquid electrode were also made with Li [16] or Mg [17] as RA.

However, few studies have been conducted in fluoride salts. In $LiF–BeF_2$, Bi–Li alloy in contact with rare earths and actinides was used to evaluate the kinetic parameters [18] and distribution coefficients [18,19]; in the same solvent, Bi, Sn, Cd and Zn were examined as metal phases [20]. More recently, $LiF–AlF_3$ eutectic mixture with Al as RA was identified to be very promising [21,22].

All the authors agree that the separation performances are highly influenced by the choice of the metallic cathode. Fundamental investigations are thus needed to select good candidates to be used in both electrorefining and reductive extraction processes.

Liquid metallic cathodes such as gallium (Ga), lead (Pb), tin (Sn), antimony (Sb) and bismuth (Bi) in molten $LiF–CaF_2$ at 850 °C and LiF–NaF at 750 °C were examined. As preamble, the main physico-chemical properties of metals are presented and discussed. The first part is dedicated to the electrochemical behaviour of the liquid metals, investigated by linear sweep voltammetry, to sort their reactivity and nobility. Then, the in situ generation of electrodes, composed of Bi liquid metal and RA (Li, Na, Ca), was considered for reductive extraction process in $LiF–CaF_2$ at 850 °C and LiF–NaF at 750 °C. Galvanostatic electrolyses were performed on Bi and cathodes were analysed by ICP-AES. From these data, general relationships between the amount of species and the electrolysis potential were found.

2. Experimental

2.1. The cell

The cell was a vitreous carbon crucible placed in a cylindrical vessel made of refractory steel and closed by a stainless steel lid cooled by circulating water. The inside part of the walls was protected against fluoride vapours by a graphite liner. The experiments were performed under an inert argon atmosphere (less than one ppm O_2), previously dehydrated and deoxygenated using a purification cartridge (Air Liquide). The cell was heated using a programmable furnace and the temperatures were measured using a chromel–alumel thermocouple.

The electrolytic bath consisted of an eutectic $LiF–CaF_2$ (Carlo Erba Reagents 99.99%) mixture (79.5/20.5 M ratio) and LiF–NaF (Carlo Erba Reagents 99.99%) mixture (60/40 M ratio), initially dehydrated by heating under vacuum (10^{-5} bar) to its melting point for 72 h.

2.2. Electrodes

Molybdenum wire (Goodfellow 99.99%, 1 mm diameter) was used as a solid working electrode. Metallic pellets of Bi, Sb, Pb, and Sn and liquid metallic Ga (Goodfellow 99.99%) were used for the liquid working electrodes. The auxiliary electrode was a vitreous carbon (Mersen spectroscopic quality) rod (3 mm diameter) with a large surface area (2.5 cm^2). The surface area of the solid working electrode was determined after each experiment by measuring the immersion depth in the bath.

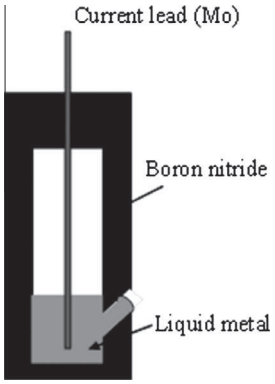

Fig. 1. Scheme of a typical liquid metal electrode.

The potentials were referred to a tantalum reference electrode: K_2TaF_7 (2 mol%) and a Ta wire (Goodfellow 99.99%) enclosed in boron nitride (BN, AX05 grade), in contact with the solution through a 0.2 mm hole.

Liquid electrodes (around 1.6 g of metal) were contained in boron nitride (BN, AX05 grade) and a scheme of the assembly is presented in Fig. 1. The current feeder was a molybdenum wire (1 mm diameter) immersed in the liquid metal and the contact between the salt and the metal was done by a hole in the BN wall (surface area of contact: 0.41 cm^2).

2.3. Techniques

The electrochemical study and the electrolyses were performed with an Autolab PGSTAT30 potentiostat/galvanostat controlled with the GPES 4.9 software; cyclic voltammetry, linear sweep voltammetry and galvanostatic electrolyses were used.

Bi, Li, Na and Ca contents in the liquid cathode were measured, after dissolution in an equimolar mixture of pure nitric and hydrochloric acids, using Inductively Coupled Plasma–Atomic Emission Spectroscopy (ICP–AES, HORIBA Ultima 2).

3. Results and discussion

3.1. Liquid metal selection

The handling of liquid metal is constraining as the liquid electrode container has to be chemically inert to both fluoride salts and liquid metals, and also insulating as the cathode is polarized. Only few materials fulfil these criteria and among of them, boron nitride was chosen. In order to select metals for liquid electrodes, some conditions should be respected:

- The metal has to be liquid at the operating temperature for both fluoride solvent: 850 °C in $LiF–CaF_2$ and 750 °C in LiF–NaF. Moreover, the metal should not boil for a better use of the liquid cathode. These limitations define a range of temperature where the working temperature should be between the melting point and the boiling point of the metallic element.
- A large difference in density at the operating temperature is required between the metal and the electrolyte. In our experiment, the liquid metal has to be denser than the molten fluorides, which are 2.04 g cm^{-3} for $LiF–CaF_2$ at 850 °C and 1.96 g cm^{-3} for LiF–NaF at 750 °C [23].
- As the liquid metal is in equilibrium with its saturated vapour pressure, a low vapour pressure at operating temperature is requisite to avoid metal distillation.

Melting and boiling points, density and vapour pressure of bismuth (Bi), gallium (Ga), lead (Pb), antimony (Sb) and tin (Sn) are gathered Table 1: these elements strictly respect each conditions and were used as liquid metallic electrode.

3.2. Electrochemical properties of liquid metals

In this part, the behaviour of liquid electrodes was studied by electrochemical measurements (oxidation and reduction). Linear sweep voltammetry was performed at 10 mV s^{-1} in $LiF–CaF_2$ at 850 °C and in LiF–NaF at 750 °C on Ga, Pb, Sn, Sb, Bi, and Mo. An

Table 1
Main physico-chemical properties of metals used as cathode: Bi, Ga, Pb, Sb and Sn.

Metal	Bi	Ga	Pb	Sb	Sn
Melting point (°C)	271.4	29.76	327.46	630.63	231.93
Boiling point (°C)	1564	2204	1749	1587	2602
Density at 25 °C	9.78	5.91	11.34	6.70	7.36
Density at m.p.	10.05	6.09	10.66	6.53	5.77
Vapour pressure (Pa)	10 (768 °C)	1 (1037 °C)	10 (815 °C)	100 (738 °C)	1 (1224 °C)

overlay of these voltammograms is given in Fig. 2 for LiF–CaF_2 and Fig. 3 for LiF–NaF.

3.2.1. Reduction part analysis

In the reduction part for both eutectic mixtures, the solvent reduction takes place at a more positive potential on liquid electrodes than on an inert Mo electrode. These underpotential depositions are due to alloy formation between the metallic electrode M and the metal deposition from the solvent, to form M–Na and/or M–Li alloys in LiF–NaF and M–Li and/or M–Ca alloys in LiF–CaF_2. The reducing ability of the metal (or reactivity scale) was thus determined by measuring the reduction equilibrium potential ($E_{I=0}$) of the solvent. By sorting these potentials, a reactivity series was found to be the same in both fluoride salts, from the highest to the lowest reactivity:

Sb > Bi > Pb > Sn > Ga > Mo

Thus, within these five electrodes, the most reactive one is antimony and the less reactive gallium.

3.2.2. Oxidation part analysis

In the oxidation part, by recording the value of the equilibrium potential ($E_{I=0}$) of the metal oxidation, the relative nobility of the material was obtained and the same trend was also observed in both fluoride salts:

Ga < Sn < Pb < Sb < Bi-Mo

Bismuth and molybdenum oxidation occurs at the same potential and bismuth appears to be the noblest metal.

3.2.3. Electroactivity domain

From these data, the electroactivity domain (EAD), corresponding to the potential zone where the electrode does not record any current, can be evaluated as:

$$\mathrm{EAD} = E_{I=0}(\text{oxidation}) - E_{I=0}(\text{reduction}) \quad (1)$$

Table 2 gathers the electroactivity domains for the different liquid electrodes in LiF–NaF and LiF–CaF_2 and the largest one is observed on bismuth in LiF–CaF_2 and the narrowest domain on gallium in LiF–NaF.

This electroactivity domain is crucial for electrolysis processes; the reduction potential of the solvent represents the extraction limit of the solute, hence fixing its extraction yield. By comparing the reduction potentials of solute and solvent, the efficiency of the extraction process can be evaluated.

3.3. In situ formation of metal-reducing agent electrodes

In this paragraph, the in situ generation of reactive cathodes used in the liquid–liquid reductive extraction process was examined. The electrolytic production of reactive alloyed cathodes with a controlled amount of reducing agent (RA) was tested; only bismuth cathode was explored in LiF–NaF at 750 °C and LiF–CaF_2 at 850 °C.

3.3.1. Galvanostatic electrolyses on liquid Bi

To control the RA insertion rate in liquid Bi, galvanostatic electrolyses were performed. Experimental conditions were a constant current fixed at −80 mA and four different electrolysis times, from 1425 s to 16,000 s. The corresponding electrical charges were:

114 C, 256 C, 456 C and 864 C in LiF–CaF_2

320 C, 640 C, 920 C and 1280 C in LiF–NaF

The coulometric curves (E vs. Q) are presented in Figs. 4 and 5 for LiF–CaF_2 and LiF–NaF respectively. In both media, the same shape is obtained, meaning a constant reduction rate: no brutal variation of the potential is observed, showing a continuous insertion of the solvent elements into Bi. Moreover, the coulometric curves are perfectly superimposed for the same applied current,

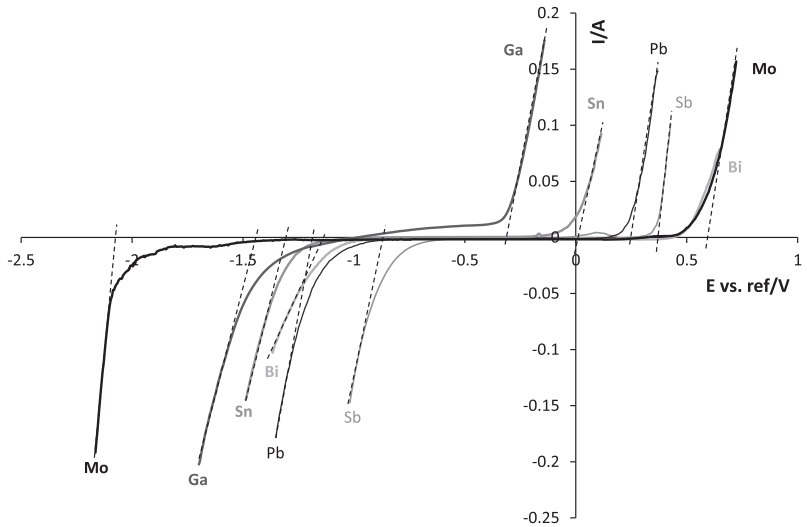

Fig. 2. Linear sweep voltammetries at 10 mV s^{-1} on liquid metal cathodes (Ga, Pb, Sn, Sb, Bi) and Mo in LiF–CaF_2 at 850 °C.

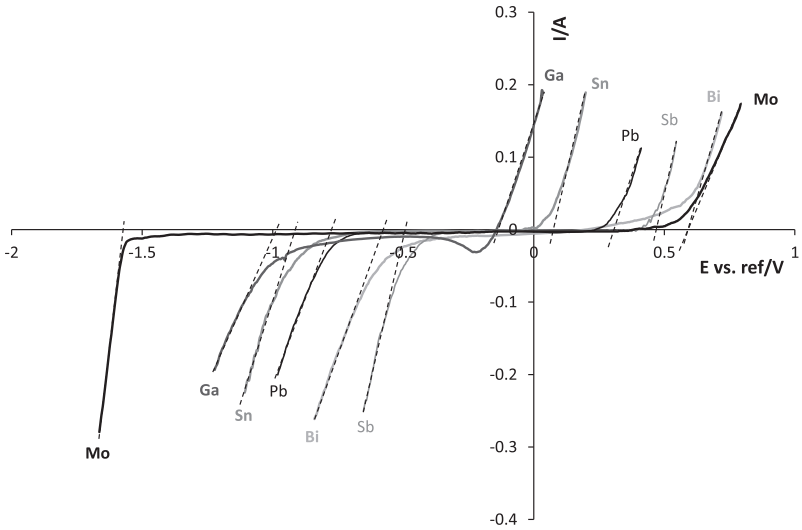

Fig. 3. Linear sweep voltammetries at 10 mV s^{-1} on liquid metal cathodes (Ga, Pb, Sn, Sb, Bi) and Mo in LiF–NaF at 750 °C.

Table 2
Electroactivity domains measured on Bi, Ga, Pb, Sb and Sn in LiF–CaF_2 at 850 °C and LiF–NaF at 750 °C.

Metal	Bi (V)	Ga (V)	Pb (V)	Sb (V)	Sn (V)
LiF–CaF_2	1.660	1.155	1.430	1.240	1.305
LiF–NaF	1.214	0.829	1.158	0.982	1.033

demonstrating the reproducibility of liquid electrode fabrication. It is also observed that the electrolysis potential decreases with the electrical charge passed during the experiment, thus with an increase of RA content (Li, Na and Ca) in the Bi pool, as described in Eq. (2):

$$E_{\text{electro}} = \eta + E^{0}_{RA^{+}/RA} + \frac{RT}{nF}\ln\left(\frac{a_{RA^{+}(\text{solution})}}{a_{RA}\text{in Bi—RA}}\right) \quad (2)$$

where η is the overpotential (V), $E°$ the standard potential (V), R the ideal gas constant (J K^{-1} mol^{-1}), T the absolute temperature (K), n the number of exchanged electrons, F the Faraday constant (C mol^{-1}) and a the species activity.

During electrolysis runs, RA^{+} activity is assumed to be constant (solvent) whereas the activity of RA in Bi–RA alloy increases: the activity ratio tends to decrease, thus the potential during electrolysis decreases with an increase of RA into the Bi pool.

To correlate the electrolysis potential and the RA content in the electrogenerated reactive electrode, elemental analyses are required.

3.3.2. Elemental analysis of reactive Bi cathodes

After galvanostatic electrolyses, liquid cathodes were cooled down under Ar atmosphere and quickly dissolved in an equimolar mixture of pure nitric and hydrochloric acids. Li, Na, Ca and Bi elements were determined by ICP–AES and analytical results are gathered in Tables 3 and 4 for LiF–NaF and LiF–CaF_2 respectively.

In LiF–NaF, the solvent reduction is presumed to be the Na formation on inert electrode, according to thermodynamic prediction. It is observed in Table 3 that Na is mainly deposited and a ratio of around 8 between the Na and the Li content in the Bi alloy is obtained, meaning that Na and Li are both reduced but with different reduction rates:

$$Bi + Na^{+} + e^{-} = BiNa \quad (3)$$

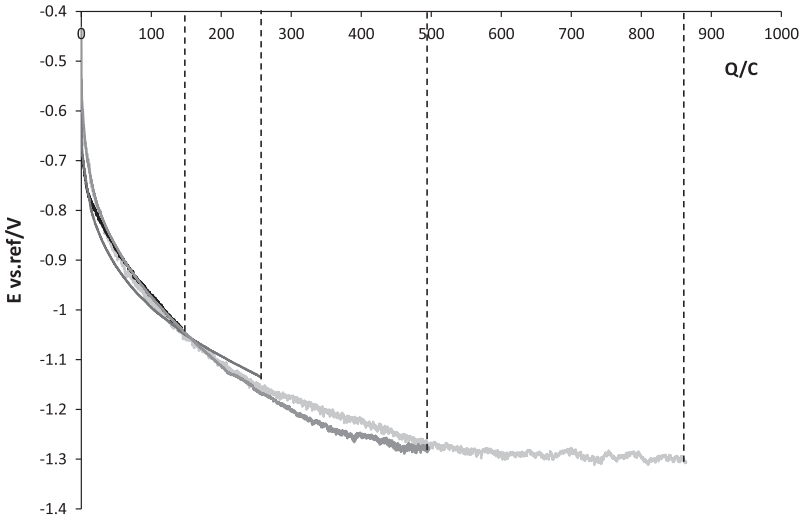

Fig. 4. Coulometric curves in galvanostatic mode (I = −80 mA) on Bi in LiF–CaF_2 at 850 °C obtained for different electrical charges: 114 C, 256 C, 496 C and 864 C.

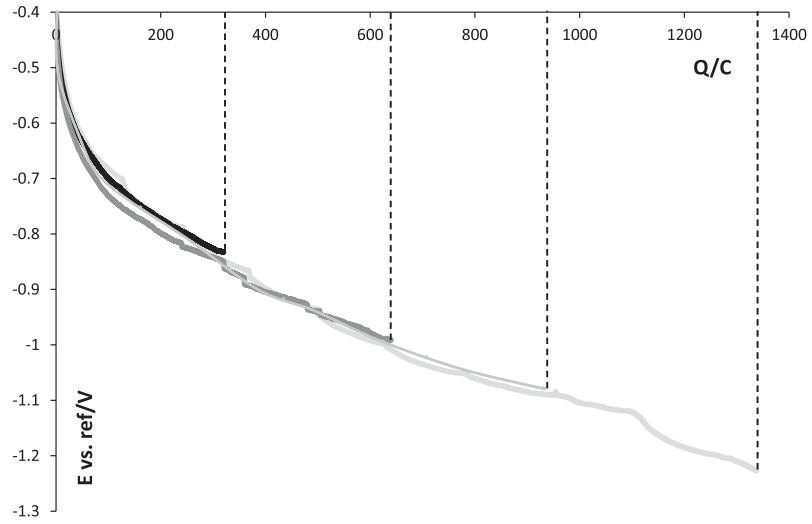

Fig. 5. Coulometric curves in galvanostatic mode ($I = -80$ mA) on Bi in LiF–NaF at 750 °C obtained for different electrical charges: 320 C, 640 C, 920 C, and 1280 C.

Table 3
Molar fractions of Li and Na obtained after electrolysis on Bi in LiF–NaF by ICP measurements.

Q (C)	320	640	920	1280

Table 4
Molar fractions of Li and Ca obtained after electrolysis on Bi in LiF–CaF_2 by ICP measurements.

Q (C)	114	256	456	864
x_{Li}	0.061	0.103	0.167	0.204
x_{Ca}	0.052	0.092	0.154	0.192

$$Bi + Li^{+} + e^{-} = BiLi \quad (4)$$

Thermodynamically, the solvent reaction in LiF–CaF_2 on an inert electrode is assumed to be the Li formation. From ICP–AES measurements, Ca and Li are simultaneously inserted into the Bi pool with the same reduction rate as their molar fraction ratio is 0.9. However, comparing the number of exchanged electrons, around two thirds of the intensity was used to deposit Ca in the Bi liquid electrode.

$$Bi + Li^{+} + e^{-} = BiLi \quad (5)$$

$$Bi + Ca^{2+} + 2e^{-} = BiCa \quad (6)$$

The correlation between the electrolysis potential and the RA activity in the liquid metal is shown in Eq. (2). As the activity is directly proportional to the molar fraction, the potential at the end of the electrolysis was plotted versus the logarithm of the RA molar fractions. In Figs. 6 and 7, linear relationships are observed in both solvent (cf. Eq. (2)).

The solvent species reduction occurs simultaneously (Li and Na, Li and Ca) with a constant insertion rate; a global molar fraction x_{global} can be thus calculated as the sum of the molar fraction of each species in Bi, weighted by the number of exchanged electrons. x_{global} is then the molar fraction of one equivalent RA which exchanges one electron. By taking into account the RA oxidation state, it is calculated as:

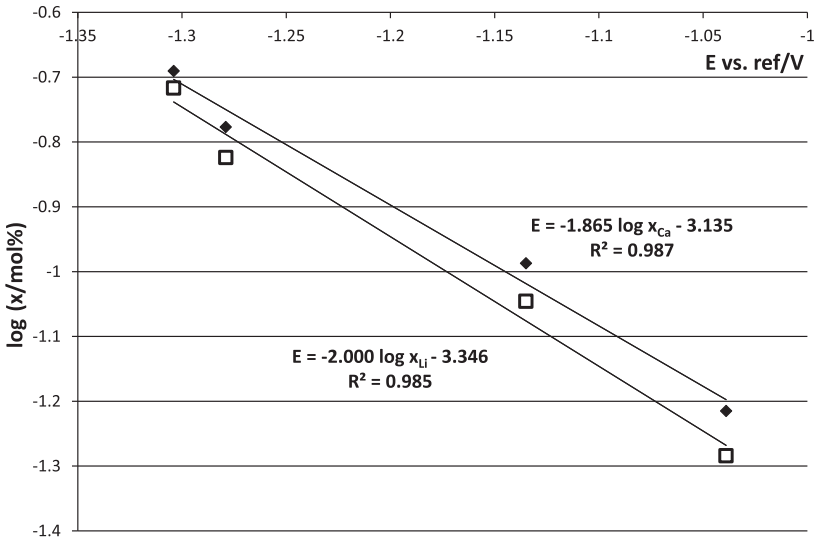

Fig. 6. Linear relationships between the electrode potential during the electrolysis and the logarithm of the molar fraction of Li (square) and Ca (rhombus) in LiF–CaF_2 at 850 °C.

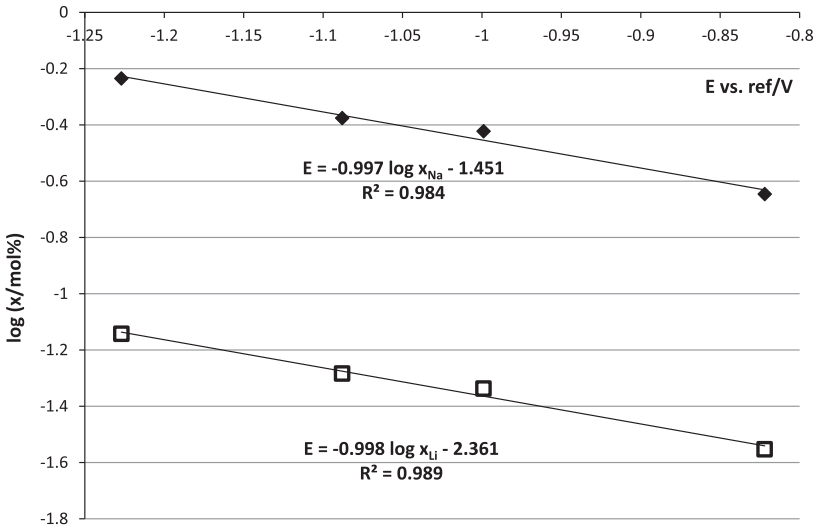

Fig. 7. Linear relationships between the electrode potential during the electrolysis and the logarithm of the molar fraction of Li (square) and Na (rhombus) in LiF–NaF at 750 °C.

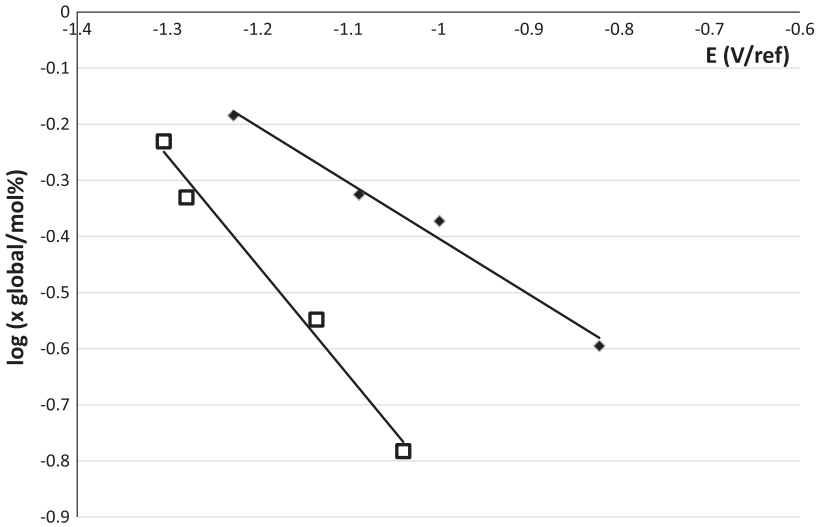

Fig. 8. Linear relationships between the electrode potential during the electrolysis and the logarithm of the global molar fraction in LiF–CaF_2 at 850 °C (square) and in LiF–NaF at 750 °C (rhombus).

$$\text{In LiF—CaF}_2 \quad x_{\text{global}} = 2 * x_{\text{Ca}} + x_{\text{Li}} \tag{7}$$

$$\text{In LiF—NaF} \quad x_{\text{global}} = x_{\text{Na}} + x_{\text{Li}} \tag{8}$$

In Fig. 8 is represented the linear regressions between the logarithm of this global molar fraction and the electrolysis potential in both solvent:

$$\text{In LiF—CaF}_2\ (850^{\circ}\text{C}) \quad \log x_{\text{global}} = -1.951E_{\text{electro}} - 2.793 \tag{9}$$

$$\text{In LiF—NaF}\ (750^{\circ}\text{C}) \quad \log x_{\text{global}} = -0.997E_{\text{electro}} - 1.400 \tag{10}$$

The RA global amount in the Bi pool can be thus controlled directly through the electrode potential during galvanostatic electrolysis. The preparation of reactive cathodes with a defined Bi–RA composition was thus demonstrated.

4. Conclusion

Selection criteria of liquid metallic electrodes were firstly exposed and their use requires: a liquid state and a low vapour pressure at the operating temperature, and a density higher than the solvent. First of all, investigations on the selected liquid electrodes (Pb, Sn, Ga, Sb, and Bi) were performed in LiF–NaF (750 °C) and LiF–CaF_2 (850 °C). Thanks to electrochemical measurements, linear sweep voltammetries allowed to sort the nobility and reactivity of the different metals. The same trend was observed in both solvent, where Ga is the most reactive and Bi the noblest. From these data, the extraction yield of a solute can be estimated. Then, in situ formation of reactive Bi-reducing agent (RA) electrode was also studied. After electrolyses runs and ICP-AES analyses, it was found that in LiF–CaF_2, Li and Ca were simultaneously deposited on bismuth with the same reduction rate, whereas in LiF–NaF, Na^+ was reduced 8 times more than Li^+. Finally, linear relationships between the electrolysis potential and the logarithm of the RA molar fraction inside the bismuth pool were found for each single species. A global RA molar fraction, weighted by the number of exchanged electrons, was defined and linear relationships between the logarithm of this value and the electrolysis potential were obtained. Bi reactive cathodes with a controlled quantity of

reducing agent can be produced in galvanostatic conditions by fixing the potential at the end of the electrolysis.

References

[1] Actinide and Fission Product partitioning and Transmutation, Status and Assessment report, NEA/OCDE, 1999.

[2] P. Masset, D. Bottomley, R. Konings, R. Malmbeck, J. Serp, J.P. Glatz, Electrochemistry of uranium in molten LiCl–KCl eutectic, J. Electrochem. Soc. 152 (6) (2005) A1109–A1115.

[3] J.C. Hesson, L. Burris, Uranium diffusivity in liquid cadmium, Trans. Metall. Soc. AIME 227 (1963) 571–581.

[4] T. Kato, T. Inoue, T. Iwai, Y. Arai, Separation behaviors of actinides from rare-earths in molten electrorefining using saturated liquid cadmium cathode, J. Nucl. Mater. 357 (2006) 105–114.

[5] M. Iizuka, K. Uozumi, T. Inoue, T. Iwai, O. Shirai, Y. Arai, Behavior of plutonium and americium at liquid cadmium cathode in molten LiCl–KCl electrolyte, J. Nucl. Mater. 299 (2001) 32–42.

[6] T. Koyama, M. Iizuka, Y. Shoji, R. Fujita, H. Tanaka, T. Kobayashi, M. Tokiwai, An experimental study of molten salt electrorefining of uranium using solid iron cathode and liquid cadmium cathode for development of pyrometallurgical reprocessing, J. Nucl. Sci. Technol. 34 (4) (1997) 384–393.

[7] M. Iizuka, T. Koyama, N. Kondo, R. Fujita, H. Tanaka, Actinides recovery from molten salt/liquid metal system by electrochemical methods, J. Nucl. Mater. 247 (1997) 183–190.

[8] J.J. Laidler, J.E. Battles, W.E. Miller, J.P. Ackerman, E.L. Carls, Development of pyroprocessing technology, Prog. Nucl. Energy 31 (1997) 131–140.

[9] J.J. Roy, L.F. Grantham, D.L. Grimmett, S.P. Fusselman, C.L. Krueger, T.S. Storvick, T. Inoue, Y. Sakamura, N. Takahashi, Thermodynamic properties of U, Np, Pu and Am in molten LiCl–KCl eutectic and liquid cadmium, J. Electrochem. Soc. 143 (8) (1996) 2487–2492.

[10] J.P. Ackerman, J.L. Settle, Partition of lanthanum and neodymium metals and chlorides salts between cadmium and molten LiCl–KCl eutectic, J. Alloys Compd. 177 (1991) 129–141.

[11] Y.S. Hwang, M.S. Jeong, S.W. Park, Current status on the nuclear back-end fuel cycle R&D in Korea, Prog. Nucl. Energy 49 (2007) 463–476.

[12] J.B. Shim, J.H. Lee, B.H. Ahn, M.S. Woo, B.G. Lee, E.H. Kim, H.S. Park, J.H. Yoo, The electrodeposition and rare earths reduction in the molten salt actinides recovery systems using liquid metal, in: Proceedings of Global 2005, Tsukuba Japan, paper 216, 2005.

[13] M. Kurata, Y. Sakamura, T. Matsui, Thermodynamic quantities of actinides and rare earth elements in liquid bismuth and cadmium, J. Alloys Compd. 234 (1996) 83–92.

[14] H. Moriyama, D. Yamada, K. Moritani, T. Sasaki, I. Takagi, K. Kinoshita, H. Yamana, Reductive extraction kinetics of actinide and lanthanide elements in molten chloride and liquid cadmium system, J. Alloys Compd. 408–412 (2006) 1003–1007.

[15] M. Kurata, Y. Sakamura, T. Hijikata, K. Kinoshita, Distribution behaviour of uranium, neptunium, rare-earth elements (Y, La, Ce, Nd, Sm, Eu, Gd) and alkaline-earth metals (Sr, Ba) between molten LiCl–KCl eutectic salt and liquid cadmium, J. Nucl. Mater. 227 (1995) 110–121.

[16] H. Moriyama, H. Yamana, S. Nishikawa, S. Shibata, N. Wakayama, Y. Miyashita, K. Moritani, T. Mitsugashira, Thermodynamics of reductive extraction of actinides and lanthanides from molten chloride salt into liquid metal, J. Alloys Compd. 271–273 (1998) 587–591.

[17] I. Johnson, The thermodynamics of pyrochemical processes for liquid metal reactor fuel cycles, J. Nucl. Mater. 154 (1988) 169–180.

[18] H. Moriyama, M. Miyazaki, Y. Asaoka, K. Moritani, J. Oishi, Kinetics of reductive extraction of actinide and lanthanide elements from molten fluoride into liquid bismuth, J. Nucl. Mater. 182 (1991) 113–117.

[19] L.M. Ferris, J.C. Mailen, F.J. Smith, Chemistry and thermodynamics of the distribution of lanthanide and actinide elements between molten LiF–BeF_2 and liquid bismuth solutions, J. Inorg. Nucl. Chem. 33 (5) (1971) 1325–1335.

[20] H. Moriyama, T. Seshimo, K. Moritani, Y. Ito, T. Mitsugashira, Reductive extraction behaviour of actinide and lanthanide elements in molten salt and liquid metal binary phase diagram, J. Alloys Compd. 213–214 (1994) 354–359.

[21] O. Conocar, N. Douyère, J.P. Glatz, J. Lacquement, R. Malmbeck, J. Serp, Promising pyrochemical actinide/lanthanide separation processes using aluminium, Nucl. Sci. Eng. 153 (2006) 253–261.

[22] O. Conocar, N. Douyère, J. Lacquement, Distribution of actinides and lanthanides in a molten fluoride/liquid aluminium alloy system, J. Alloys Compd. 389 (2005) 29–33.

[23] G.J. Janz, Molten salts Handbook, Academic Press Inc., London, 1967.